

Magnetic Monopoles, Center Vortices, Confinement and Topology of Gauge Fields¹

H. Reinhardt, M. Engelhardt, K. Langfeld, M. Quandt, A. Schäfer

Institut für Theoretische Physik

Universität Tübingen, Auf der Morgenstelle 14

D-72076 Tübingen, Germany

The vortex picture of confinement is studied. The deconfinement phase transition is explained as a transition from a phase in which vortices percolate to a phase of small vortices. Lattice results are presented in support of this scenario. Furthermore the topological properties of magnetic monopoles and center vortices arising, respectively, in Abelian and center gauges are studied in continuum Yang-Mills-theory. For this purpose the continuum analog of the maximum center gauge is constructed.

1 Introduction

Recent lattice calculations have given strong evidence for two confinement scenarios:

1. the dual Meissner effect [1], which is based on a condensate of magnetic monopoles in the QCD vacuum and 2. the center vortex picture [2], where the vacuum consists of a condensate of magnetic flux tubes which are closed due to the Bianchi identity. There are also lattice calculations which indicate that the spontaneous breaking of chiral symmetry, which can be related to the topology of gauge fields, is caused by these objects, i.e. by either magnetic monopoles [5] or center vortices [6]. In this talk we would like to discuss the confinement and topological properties of magnetic monopoles and center vortices. We will first discuss the two confinement scenarios based on magnetic monopoles and vortices, respectively, and subsequently investigate the topological properties of these objects. In particular, we will study the nature of the deconfinement phase transition in the center vortex picture. We will also show that in Polyakov gauge the magnetic monopoles completely account for the non-trivial topology of the gauge fields. Subsequently, we will extend the notion of center vortices to the continuum. We will present the continuum analog of the maximum center gauge fixing and the Pontryagin index of center vortices.

2 Confinement

The magnetic monopoles arise in Yang-Mills-Theories in the so called Abelian gauges [7]. Recent lattice calculations have shown that below a critical temperature

¹invited talk given by H. Reinhardt on the Int. Workshop "Hadrons 1999", Coimbra, 10.-15. Sept. 1999

T_C these monopoles are condensed [10] and give rise to the dual Meißner effect. In particular in the so called maximal Abelian gauge where all links are made as diagonal as possible, one observes Abelian and monopole dominance in the string tension [1]. However, very recent lattice calculations [11] also show that the Yang-Mills ground state does not look like a Coulombic monopole gas but rather indicate a collimation of magnetic flux, which is consistent with the center vortex picture of confinement, proposed in refs. [12], [13], [15], [14].

Center vortices represent closed magnetic flux lines in three space dimensions, describing closed two-dimensional world-sheets in four space-time dimensions. The magnetic flux represented by the vortices is furthermore quantized such that a Wilson loop linking vortex flux takes a value corresponding to a nontrivial center element of the gauge group. In the case of $SU(2)$ colour the only such element is (-1) . For N colours, there are $N - 1$ different possible vortex fluxes corresponding to the $N - 1$ nontrivial center elements of $SU(N)$. Center vortices can be regarded as a fraction of a Dirac string: N superimposed center vortices form an unobservable Dirac string.

Consider an ensemble of center vortex configurations in which the vortices are distributed randomly, specifically such that intersection points of vortices with a given two-dimensional plane in space-time are found at random, uncorrelated locations. In such an ensemble, confinement results in a very simple manner. Let the universe be a cube of length L , and consider a two-dimensional slice of this universe of area L^2 , with a Wilson loop embedded into it, circumscribing an area A . On this plane, distribute N vortex intersection points at random, cf. Fig. 1 (left). According to the specification above, each of these points contributes a factor (-1) to the value of the Wilson loop if it falls within the area A spanned by the loop; the probability for this to occur for any given point is A/L^2 .

The expectation value of the Wilson loop is readily evaluated in this simple model. The probability that n of the N vortex intersection points fall within the area A is binomial, and, since the Wilson loop takes the value $(-1)^n$ in the presence of n intersection points within the area A , its expectation value is

$$\begin{aligned} \langle W \rangle &= \sum_{n=0}^N (-1)^n \binom{N}{n} \left(\frac{A}{L^2} \right)^n \left(1 - \frac{A}{L^2} \right)^{N-n} \\ &= \left(1 - \frac{2\rho A}{N} \right)^N \xrightarrow{N \rightarrow \infty} \exp(-2\rho A), \end{aligned} \quad (1)$$

where in the last step, the size of the universe L has been sent to infinity while leaving the planar density $\rho = N/L^2$ of vortex intersection points constant. Thus, one obtains an area law for the Wilson loop, with the string tension $\sigma_{vm} = 2\rho$.

In fact, in lattice calculations the vortex area density ρ has been shown to obey the proper scaling behaviour [3] as dictated by the renormalization group and thus represents a physical observable. Using a string tension of

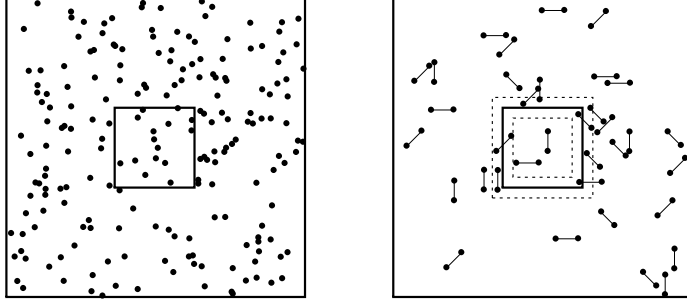


Figure 1: Two-dimensional plane of a random vortex gas with a planar Wilson loop. The dots represent the intersection points of the vortices with the plane considered. Left figure: confining vortex ensemble of uncorrelated intersection points. Right figure: deconfining vortex ensemble in which the intersection points occur pairwise within a distance d away from each other. (The intersection points of a pair are connected by a line.)

$\sigma \sim (440 \text{ MeV})^2$ as input one finds $\rho \approx 3.4 F^{-2}$ corresponding to a string tension $\sigma_{rvm} = (521 \text{ MeV})^2$ in the random model above which overestimates the input value. This overabundance of string tension can be easily understood by noticing that there are both dynamical [17] and kinematical correlations between the vortex intersection points, which have been discarded in the random vortex model considered above, which assumes that all intersection points are completely random, i.e. uncorrelated. This is, however, not true since the vortices are closed loops in $D = 3$ or closed surfaces in $D = 4$. Therefore the intersection points in the plane of the Wilson loops come in pairs. But a pair of intersection points does not (non-trivially) contribute to the Wilson loop. Only for large vortices exceeding the size of the Wilson loop the intersection points inside the Wilson loop are uncorrelated and can contribute (-1) . On the other hand all vortices contribute to the area vortex density ρ measured on the lattice. This effect leads to a lower value of the string tension than the value $\sigma_{rvm} = 2\rho$ resulting from the random vortex model.

3 Deconfinement

The above presented vortex picture of confinement naturally explains also the deconfinement transition as a transition from a phase of large vortices percolating

throughout space-time to a phase of small vortices in a sense to be specified more precisely below. Indeed, assume that all vortices have a maximal size d . Then only the intersection points in a strip of width d along the perimeter of the Wilson loop can randomly contribute (-1) , (while other intersection points come in pairs and hence do not contribute). The expectation value of the Wilson loop is then still given by eq. (1), however, with the full area A of the Wilson loop replaced by the area of the strip of width d along the perimeter P of the Wilson loop, $d \cdot P$, resulting in a perimeter law

$$\langle W \rangle = \exp(-2\rho dP) \quad (2)$$

implying deconfinement. This picture of the deconfinement phase transition arising in the random vortex model as a transition from a phase of percolating vortices to a phase of small vortices is supported by the lattice calculations. Fig. 2 shows the vortex matter distribution as function of the vortex cluster extension at various temperatures for a 3-dimensional slice resulting from the 4-dim. lattice by omitting one spatial direction[18], see also ref. [17]. Far below the critical temperature T_C of the deconfinement phase transition a dominant portion of the vortex matter is contained in a big cluster extending over the whole lattice universe. As the temperature rises smaller clusters are more and more formed and well above the deconfinement phase transition large vortices have ceased to exist, the connectivity of the clusters is lost and all vortex matter being contained in small clusters.

If one analyzes the small vortex clusters dominating the deconfined phase in more detail, one finds that a large part of these vortices wind in the (Euclidean) temporal direction, i.e. the space-time direction whose extension is identified with the inverse temperature. Therefore, one finds that the typical configurations in the two phases can be characterized as displayed in Fig. 3 in a three-dimensional slice of space-time, where one space direction has been left away. Note that Fig. 3 also furnishes an explanation of the spatial string tension in the deconfined phase. A spatial Wilson loop embedded into Fig. 3 (right) can exhibit an area law since intersection points of winding vortices with the minimal area spanned by the loop can occur in an uncorrelated fashion despite those vortices having small extension. Note also the dual nature of this (magnetic) picture as compared with electric flux models [19]. In such models, electric flux percolates in the *deconfined* phase, while it does not percolate in the confining phase.

4 Magnetic monopoles and topology

Spontaneous breaking of chiral symmetry can be triggered by topologically non-trivial gauge fields, which give rise to zero modes of the quarks [21]. Magnetic

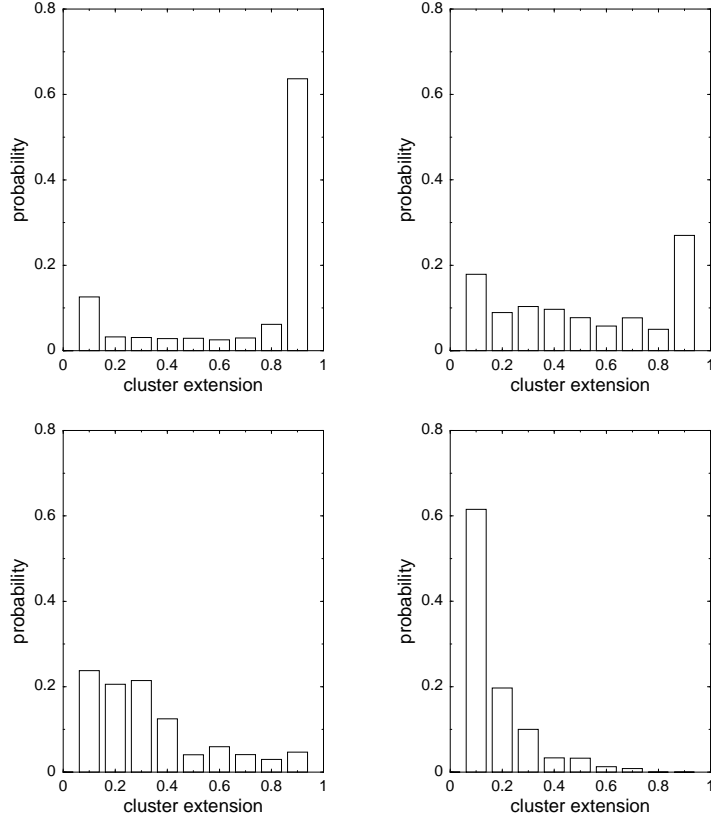


Figure 2: Vortex material distributions.

monopoles and percolated vortices are long range fields and should hence be relevant for the global topological properties.

Topological properties of gauge configurations as measured by the Pontryagin index

$$\nu = \frac{-1}{16\pi^2} \int Tr F_{\mu\nu} \tilde{F}_{\mu\nu} = \frac{1}{4\pi^2} \int d^3x \vec{E}(x) \vec{B}(x) \quad (3)$$

are preferably studied in the continuum theory. For the study of the topological properties of magnetic monopoles in the continuum theory the Polyakov gauge is particularly convenient. In this gauge one diagonalizes the Polyakov loop

$$\Omega(\vec{x}) = P e^{-\int_0^T dx_0 A_0(x_0, \vec{x})} = V^\dagger \omega V \quad (4)$$

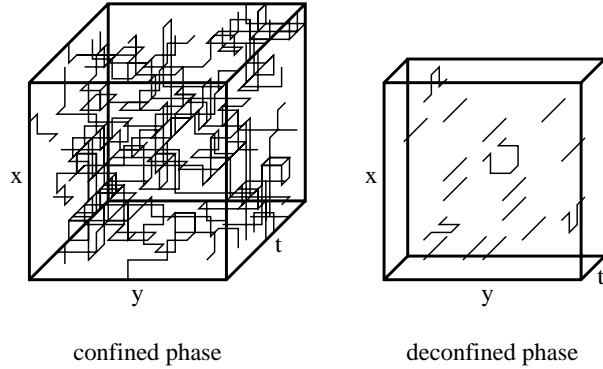


Figure 3: Typical vortex configurations in the confining (left) and the deconfined phase (right).

which fixes $V \in SU(2)/U(1)$ i.e. the coset part of the gauge group, which we assume, for simplicity, to be $SU(2)$. Magnetic monopoles arise as defects of the gauge fixing, which occur when at isolated points in space \vec{x}_i the Polyakov loop becomes a center element

$$\Omega(\vec{x}_i) = (-1)^{n_i}, \quad n_i : \text{integer} \quad (5)$$

The field $A^V = VAV^\dagger + V\partial V^\dagger$ develops then magnetic monopoles located at these points. These monopoles have topologically quantized magnetic charge [8] given by the winding number

$$m[V] \in \Pi_2(SU(2)/U(1)) \quad (6)$$

of the mapping $V(\vec{x})$ from a sphere S_2 around the magnetic monopole into the coset $SU(2)/U(1)$ of the gauge group.

In the Polyakov gauge the Pontryagin index can be exactly expressed in terms of magnetic charges [8], [22], [20]. If we assume a compact space-time manifold and that there are only point-like defects of gauge fixing, i.e magnetic monopoles are the only magnetically charged objects arising after gauge fixing, the Pontryagin index is given by [8]

$$\nu = \sum_i n_i m_i \quad (7)$$

The summation runs here over all magnetic monopoles with m_i being the magnetic charge of the monopole defined by equation (6) and the integer n_i is defined by the value of the Polyakov-loop at the monopole position (5). This relation shows that the magnetic monopoles completely account for the non-trivial topology of gauge fields, at least in the Polyakov gauge. Unfortunately, in other Abelian gauges like maximum Abelian gauge, such a simple relation

between Pontryagin index and magnetic charges is not yet known and perhaps does not exist [20]. However, in the maximum Abelian gauge correlations between instantons and monopoles have been found, in both analytical and lattice studies [5].

5 Center vortices in the continuum

On the lattice center vortices are detected by going to the maximum center gauge and subsequently projecting the links onto center elements [2]. In the maximum center gauge

$$\sum_{x,\mu} (Tr U_\mu(x))^2 \rightarrow max , \quad (8)$$

which is obviously insensitive to center gauge transformations, one exploits the gauge freedom to rotate a link variable as close as possible to a center element. Once the maximum center gauge has been implemented, center projection implies to replace all links by their closest center element. One obtains then a $Z(2)$ lattice which contains $D-1$ dimensional hypersurfaces Σ on which all links take a non-trivial center element, that is $U = -1$ in the case of $SU(2)$. The $D-2$ dimensional boundaries $\partial\Sigma$ of the hypersurfaces Σ represent the center vortices, which, when non-trivially linked to a Wilson loop, yield a center element for the latter. The notion of center vortices can be extended to the continuum theory by putting a given smooth gauge field $A_\mu(x)$ on a lattice in the standard fashion by introducing the link variables $U_\mu(x) = \exp(-aA_\mu(x))$.

A careful analysis shows that the continuum analogies of the center vortices are defined by the gauge potential [9],

$$A_\mu(x, \Sigma) = E \int_\Sigma d^{D-1} \tilde{\sigma}_\mu \delta^D(x - \bar{x}(\sigma)) \quad (9)$$

where $d^{D-1} \tilde{\sigma}_\mu$ is the dual of the $D-1$ dimensional volume element. Furthermore, the quantity $E = E_a H_a$ with H_a being the generators of the Cartan algebra represents (up to a factor of 2π) the so called co-weights which satisfy $\exp(-E) = Z \in Z(N)$. Due to this fact the Wilson-loop calculated from the gauge potential (9) becomes,

$$W[\mathcal{A}](C) = \exp(-\oint_C \mathcal{A}) = Z^{I(C, \Sigma)} \quad (10)$$

where $I(C, \Sigma)$ is the intersection number between the Wilson-loop C and the hypersurface Σ . The representation, (9), is referred to as ideal center vortex. One should emphasize that the hypersurface Σ can be arbitrarily deformed by a center gauge transformation keeping, however, its boundary $\partial\Sigma$, i.e. the

position of the center vortex, fixed. Thus for fixed $\partial\Sigma$ the dependence of the gauge potential (9) on the hypersurface itself is a gauge artifact.

The dependence on the hypersurface Σ can be removed by performing the gauge transformation

$$\varphi(x, \Sigma) = \exp(-E\Omega(x, \Sigma)) \quad (11)$$

where $\Omega(x, \Sigma)$ is the solid angle subtended by the hypersurface Σ as seen from the point x . One finds then

$$\mathcal{A}_\mu(x, \Sigma) = \varphi(x, \Sigma)\partial_\mu\varphi^\dagger(x, \Sigma) + a_\mu(x, \partial\Sigma) \quad (12)$$

where

$$a_\mu(x, \partial\Sigma) = E \int_{\partial\Sigma} d^{D-2}\tilde{\sigma}_{\mu\nu}\partial_\nu D(x - \bar{x}(\sigma)) \quad (13)$$

depends only on the vortex position $\partial\Sigma$ and is referred to as "thin vortex". Here $D(x - \bar{x}(\sigma))$ represents the Green function of the D dimensional Laplacian. In fact, one can show [9] that the thin vortex represents the transversal part of the ideal vortex $a_\mu(x, \partial\Sigma) = P_{\mu\nu}\mathcal{A}_\nu(x, \Sigma)$ where $P_{\mu\nu} = \delta_{\mu\nu} - \frac{\partial_\mu\partial_\nu}{\partial^2}$ is the usual transversal projector. A careful and lengthy analysis [9] yields that the continuum analog of the maximum center gauge fixing is defined by

$$\min_{\partial\Sigma} \min_g \int \text{Tr}(A^g - a(\partial\Sigma))^2 \quad (14)$$

where the minimization is performed with respect to all (continuum) gauge transformations $g \in SU(2)/Z(2)$ (which represent per se coset gauge transformations) and with respect to all vortex surfaces $\partial\Sigma$. For fixed thin center vortex field configuration $a(\partial\Sigma)$ minimization with respect to the continuum gauge transformation g yields the background gauge condition

$$[\partial_\mu + a_\mu(\partial\Sigma), A_\mu] = 0 \quad (15)$$

where the thin vortex field $a_\mu(x, \partial\Sigma)$ figures as background gauge field. One should emphasize, however, that the background field has to be dynamically determined for each given gauge field $A_\mu(x)$ and thus depends on the latter. Obviously in the absence of a vortex structure in the considered gauge field $A_\mu(x)$ the background gauge condition reduces to the Lorentz gauge $\partial_\mu A_\mu = 0$.

6 Topology of Center vortices

Once the center vortex configurations in the continuum are at our disposal, it is straightforward to calculate their Pontryagin index. In the continuum formulation where center vortices live in the Abelian subgroup by construction

the direction of the magnetic flux of the vortices is fully kept. The explicit calculation [9] shows that the Pontryagin index ν of the center vortices is given by

$$\nu = \frac{1}{4}I(\partial\Sigma, \partial\Sigma) \quad (16)$$

where $I(\partial\Sigma, \partial\Sigma)$ represents the self-intersection number of the closed vortex sheet $\partial\Sigma$ defined by

$$I(\partial\Sigma_1, \partial\Sigma_2) = \frac{1}{2} \int_{\partial\Sigma_1} d\sigma_{\mu\nu} \int_{\partial\Sigma_2} d\tilde{\sigma}_{\mu\nu} \delta^4(\bar{x}(\sigma) - \bar{x}(\sigma')) . \quad (17)$$

A careful analysis shows that for closed oriented surfaces the self intersection number vanishes. In order to have a non-trivial Pontryagin index the vortex surfaces have to be not globally oriented, i.e., they have to consist of oriented pieces. One can further show that at the border between oriented vortex patches magnetic monopole currents flow. It is these monopole currents which make the vortex sheet non-oriented since they change the orientation of the magnetic flux. Thus we obtain that even for the center vortices the non-trivial topology is generated by magnetic monopole currents flowing on the vortex sheets. This is consistent with our finding in the Polyakov gauge (see eq. (7)) where the Pontryagin index was exclusively expressed in terms of magnetic monopoles [8]. In fact, for a compact space-time manifold one can show that under certain mild assumptions the Pontryagin index can be expressed as

$$\nu = -\frac{1}{4}L(\partial\Sigma, C) , \quad (18)$$

where $L(\partial\Sigma, C)$ is the linking number between the vortex $\partial\Sigma$ and the monopole loop C on the vortex.

By implementing the maximum center gauge condition in the continuum one can derive, in an approximate fashion, an effective vortex theory [9], where the vortex action can be calculated in a gradient expansion. The leading order gives the Nambu-Goto action while in higher orders curvature terms appear. A model based on such an effective vortex action, in fact, reproduces the gross features of the center vortex picture found in numerical Yang-Mills lattice simulations.

Acknowledgment:

This work was supported in part by the DFG-Re 856/4-1 and DFG-En 415/1-1.

Literatur

- [1] G .S. Bali, C. Schlichter and K. Schilling, Prog. Theor. Phys. Suppl. **131** (1998) 645 (1998) and references therein.

- [2] L. Del Debbio, M. Faber, J. Greensite and S. Olejník, Phys. Rev. **D55** (1997) 2298;
L. Del Debbio, M. Faber, J. Greensite, and Š. Olejník, hep-lat/9708023;
L. Del Debbio, M. Faber, J. Giedt, J. Greensite, and Š. Olejník, Phys. Rev. **D 58**, 094501 (1998)
- [3] K. Langfeld, H. Reinhardt and O. Tennert, Phys. Lett. **B419** (1998) 317.
- [4] K. Langfeld, O. Tennert, M. Engelhardt and H. Reinhardt, Phys. Lett. **B452** (1999) 301.
- [5] S. Thurner, M. Feurstein, H. Markum and W. Sakuler, Phys. Rev. **D54** (1996) 3457;
H. Suganuma, S. Sasaki, H. Ichie, F. Araki and O. Miyamura, Nucl. Phys. Proc. Suppl. **53** (1997) 528;
S. Sasaki and O. Miyamura, Phys. Rev. **D59** (1999) 094507.
- [6] Ph. de Forcrand, M. D’Elia, Phys. Rev. Lett. **82** (1999) 4582.
- [7] G ’t Hooft, Nucl. Phys. **B190** (1981) 455
- [8] H. Reinhardt, Nucl. Phys. **B503** (1997) 505;
M. Quandt, H. Reinhardt and A. Schafke, Phys. Lett. **B446** (1999) 290.
- [9] M. Engelhardt, H. Reinhardt, hep-th/9907139
- [10] G. Di Cecio, G. Di Giacomo, G. Pafutti, M. Trigiante, Nucl. Phys. **B489** (1997) 739
A. Di Giacomo, D. Martelli, G. Pafutti, hep-lat/9905007
- [11] J. Ambjørn, J. Giedt, J. Greensite, hep-lat/9907021
- [12] G. ’t Hooft, Nucl. Phys. **B138**, 1 (1978).
- [13] J.M. Cornwall, Nucl. Phys. **B157**, 392 (1979).
- [14] H.B. Nielsen, and P. Olesen, Nucl. Phys. **B160**, 380 (1979);
J. Ambjørn, and P. Olesen, Nucl. Phys. **B170** [FS1], 60, 265 (1980);
P. Olesen, Nucl. Phys. **B200** [FS4]m 381 (1982).
- [15] G. Mack, and V.B. Petkova, Ann. Phys. (NY) **123**, 442 (1979)
G. Mack, and V.B. Petkova, Ann. Phys. (NY) **125**, 117 (1980);
G. Mack, Phys. Rev. Lett **45**, 1378 (1980).
- [16] E.T. Tomboulis, Phys. Rev. **D 23**, 2371 (1981);
E.T. Tomboulis, Phys. Lett. **B303**, 103 (1993).
- [17] M. Engelhardt, K. Langfeld, H. Reinhardt, O. Tennert, Phys. Lett. **B 431** (1998) 141.

- [18] M. Engelhardt, K. Langfeld, H. Reinhardt, O. Tennert, hep-lat/9904004, Phys. Rev. D, in press.
- [19] A. Patel, Nucl. Phys. **B243**, 411 (1984).
- [20] O. Jahn, hep-th/9909004.
- [21] T. Banks, A. Casher, Nucl. Phys. **B169** (1980) 103
- [22] C. Ford, U. G. Mitreuter, T. Tok, A. Wipf and J. M. Pawlowski, Ann. Phys. **269** (1998) 26
F. Lenz, O. Jahn, hep-th/9803177